



HAL
open science

A Robust Channel Head Extraction Method Based on High-Resolution Topographic Convergence, Suitable for Both Slowly and Fastly Eroding Landscapes

Aude Lurin, Odin Marc, Patrick Meunier, Sébastien Carretier

► To cite this version:

Aude Lurin, Odin Marc, Patrick Meunier, Sébastien Carretier. A Robust Channel Head Extraction Method Based on High-Resolution Topographic Convergence, Suitable for Both Slowly and Fastly Eroding Landscapes. *Journal of Geophysical Research: Earth Surface*, 2023, 128 (9), 10.1029/2022JF006999 . hal-04240230

HAL Id: hal-04240230

<https://hal.science/hal-04240230>

Submitted on 20 Oct 2023

HAL is a multi-disciplinary open access archive for the deposit and dissemination of scientific research documents, whether they are published or not. The documents may come from teaching and research institutions in France or abroad, or from public or private research centers.

L'archive ouverte pluridisciplinaire **HAL**, est destinée au dépôt et à la diffusion de documents scientifiques de niveau recherche, publiés ou non, émanant des établissements d'enseignement et de recherche français ou étrangers, des laboratoires publics ou privés.



Distributed under a Creative Commons Attribution - NonCommercial 4.0 International License



RESEARCH ARTICLE

10.1029/2022JF006999

Key Points:

- CO²CHAIN is a new channel detection method for high-resolution DEMs, based on relative thresholds of local and upstream convergence
- CO²CHAIN overall performs better than state-of-the-art methods on various basins even at high erosion rates, without recalibration
- CO²CHAIN allows to revisit and extend studies on channel heads and drainage networks in high erosion rate basins

Supporting Information:

Supporting Information may be found in the online version of this article.

Correspondence to:

A. Lurin,
aude.lurin@get.omp.eu

Citation:

Lurin, A., Marc, O., Meunier, P., & Carretier, S. (2023). A robust channel head extraction method based on high-resolution topographic convergence, suitable for both slowly and fastly eroding landscapes. *Journal of Geophysical Research: Earth Surface*, 128, e2022JF006999. <https://doi.org/10.1029/2022JF006999>

Received 10 NOV 2022

Accepted 11 AUG 2023

Author Contributions:

Conceptualization: Aude Lurin, Odin Marc

Data curation: Aude Lurin

Investigation: Aude Lurin

Methodology: Aude Lurin, Odin Marc,

Patrick Meunier, Sébastien Carretier

Software: Aude Lurin

Supervision: Odin Marc, Sébastien Carretier

Writing – original draft: Aude Lurin

Writing – review & editing: Odin Marc, Patrick Meunier, Sébastien Carretier

© 2023 The Authors.

This is an open access article under the terms of the [Creative Commons Attribution-NonCommercial License](https://creativecommons.org/licenses/by-nc/4.0/), which permits use, distribution and reproduction in any medium, provided the original work is properly cited and is not used for commercial purposes.

A Robust Channel Head Extraction Method Based on High-Resolution Topographic Convergence, Suitable for Both Slowly and Fastly Eroding Landscapes

Aude Lurin¹ , Odin Marc¹ , Patrick Meunier², and Sébastien Carretier¹ 

¹Géosciences Environnement Toulouse (GET), UMR 5563, CNRS/IRD/CNES/UPS, Observatoire Midi-Pyrénées, Toulouse, France, ²Ecole Normale Supérieure de Paris, Laboratoire de Géologie, Paris, France

Abstract Channel networks exert a key control on drainage basins shape and dynamics, including the transfer of water and sediments throughout basins, and thus hydrosedimentary hazards. Landscape dissection by channels results from the competition between hillslope processes and channelized erosion processes such as overland flow or debris flows. In contrast to fluvial channelization, the transition from hillslopes to colluvial channels remains understudied, and high-resolution LiDAR DEMs open new perspectives for the extensive extraction of channel heads. Several channel extraction methods exist but none is yet robust on fast eroding landscapes. Here we develop the CO²CHAIN method which identifies the hillslope to channel transition in drainage basins based on relative changes of local and upstream measures of flow convergence. We calibrate CO²CHAIN by fitting its results to channel head mapping made by geomorphologists in four contrasted basins in the United States and France with moderate to high erosion rates. Compared to two state-of-the-art channel extraction methods, it fits best the experts' mapping in terms of average characteristics and variability without needing to be recalibrated and does not have to implement a drainage area threshold although it imposes a length scale threshold. This allows to revisit studies on channelization that have not yet included high erosion rate basins.

Plain Language Summary Channels are carved by erosive processes such as water or debris flow. At the scale of a drainage basin, they form a channel network which impacts on the water and sediment dynamics of the basin, for example, by controlling its response to storms events in terms of flood and sediment exportation. Understanding how and where channels begin to form is thus of great interest for geomorphologists. However, in steep landscapes, channel heads are hard to identify on the field and the erosive processes acting just below channel heads are not fully understood. Therefore, more data is needed to constrain their location and geometry. High-resolution topographic data have opened up new perspectives in order to get this data. Here we present the CO²CHAIN method which automatically extracts channels from digital elevation models. CO²CHAIN is consistent with visual channel head mapping made by geomorphologists on four different catchments and seems to perform better than previous methods. This method could be used to revisit the conditions that allow channels to appear in a landscape, including fast eroding basins, and to better understand the competition between unchannelized and channelized erosion processes in these landscapes.

1. Introduction

Landscapes are shaped by different erosion processes. Together, these processes structure landscapes by creating different domains through which water and sediments transit. These are, mainly, the channelized domain, or drainage network, shaped by fluvial and debris-flow erosion, and the hillslope domain shaped by mass-wasting and diffusive erosion. The extent of the drainage network has great implications for landscapes morphology and dynamics. It controls how finely basins are dissected and the length of hillslopes (Tucker & Bras, 1998). It impacts the response of basins to rainfall events and the initiation of floods (Chorley & Morgan, 1962; Pallard et al., 2009). Finally, most (80%) of the relief of drainage basins and mountain range is supported by channels, thus they have a strong control on the relief and elevation of mountain ranges (Whipple et al., 1999). Therefore, identifying the boundaries of the channelized domain is a fundamental step for understanding how landscapes form and evolve and how sediments are produced and travel through them (Montgomery & Dietrich, 1988).

It has been observed since the beginning of the XXth century (Gilbert, 1909; Horton, 1945) that drainage networks only develop beyond a spatial scale threshold. This threshold has been interpreted as a characteristic scale at

which erosion by overland flow dominates over diffusive processes. Since then, many physically based models have been used to characterize the hillslope-channel transition quantitatively (Dietrich & Dunne, 1993). The initiation of erosion by overland flow in competition with hillslope diffusion has been explored in details (Izumi & Parker, 2000; Kirkby, 1986; Loewenherz, 1991; Smith & Bretherton, 1972; Tarboton et al., 1992; Willgoose et al., 1991), and other slope processes such as landsliding have also been considered (Dietrich et al., 2020; Roering et al., 1999). In a pioneering study, Tucker and Bras (1998) showed the importance of the nature of various processes (e.g., fluvial transport, overland flow, shallow landsliding, soil creep) acting on a landscape in controlling its morphology and in particular its drainage density. Their models suggested that each process combinations led to specific slope-area relationships and to specific relations between drainage density and erosion rate, precipitation and relief.

However, in some high erosion rate landscapes, evidence points toward the existence of a distinct channelized domain located between hillslopes and rivers, that we call hereafter the colluvial channels domain. It is periodically scoured by debris flows and does not have the same slope-area signature as the fluvial domain (DiBiase et al., 2012; Hergarten et al., 2016; Stock & Dietrich, 2003). While the stream-power erosion framework (Lague, 2014) has yield substantial insights on fluvial erosion and its impact on landscape evolution, long-term erosion in colluvial channels remain poorly understood. Only a few attempts have been made to upscale the behavior of single debris flow events and derive long-term erosion laws (McCoy et al., 2010; McGuire et al., 2022; Shelef & Hilley, 2016; Stock & Dietrich, 2006).

Perron et al. (2008, 2012) showed that the limit between fluvial channels and hillslopes is strongly dependent on fluvial erosion parameters, and the same must be true for colluvial processes. Therefore, precisely identifying channel heads is a major requirement in order to understand erosion in the colluvial channels as well as the formation and evolution of drainage networks in fastly eroding landscapes. However, there are inherent difficulties when comparing theory to data regarding channel heads. Dietrich and Dunne (1993) defined channels heads as the upslope boundary of concentrated water flow and sediment transport between definable banks. However, few channel heads follow exactly this definition. They can migrate downstream and upstream (Doyle & Harbor, 2003; Hattanji et al., 2021), or upstream channels can be discontinuous (Leopold & Miller, 1956), which makes it difficult to assess with certainty whether a channel head feature is active. Furthermore, in rapidly eroding landscapes, channel heads are mainly located on steep slopes and often hardly accessible. High-resolution DEMs may help to address these issues by allowing to identify channel heads at the basin scale and to statistically characterize them. However, this requires to define a suitable channel identification criterium since definable banks are rarely distinguishable on channels even in 1-m resolution DEMs. In this study, we define channels as zones of confined flow and consider that such areas are shaped by channelized erosion processes.

Several methods have been proposed to automatically extract drainage networks from DEMs. Two distinct families exist: “geometric” methods where topographic metrics are compared to empirical thresholds, and “process-based” methods where the topographic conditions defining the domains rely on model predictions of specific erosion processes. The most simple and used methods rely on a drainage area threshold (O’Callaghan & Mark, 1984) or on a threshold relating slope and drainage area (Montgomery & Dietrich, 1992). However, Orlandini et al. (2011) showed that these methods tended to find more channels than there actually was. The most recent process-based method, DrEICH (Clubb et al., 2014), is based on the steady-state topographic signature of the fluvial network and the chi-metrics (Perron & Royden, 2013). Thus, the DrEICH method is likely to give erroneous results in transiently adjusting basins or in steady-state catchments where colluvial channels dominate in the upper network (DiBiase et al., 2012; Hergarten et al., 2016). Geometric methods have been proposed based on combining thresholds on contour curvature, area, and slope-area as well as advanced filtering and network construction methods (Grieve, Mudd, Milodowski, et al., 2016; Passalacqua et al., 2010; Pelletier, 2013; Tarboton & Ames, 2001). However, most geometric methods have user-defined thresholds which need to be adjusted to the specificity of the studied DEM and are still often implemented together with an area or slope threshold. Sofia et al. (2011) proposed an advanced method combining two independent geometric parameters, curvature and openness, and applying statistically derived thresholds. However they found that it did not work well in high erosion catchments.

Here we present a new channel extraction method with limited need for calibration: the CO²CHAIN method (CO²Convergence and CO²centration Channel HeAd IdentificationN). This method considers channels as geomorphic features where any potential flow of water or sediment is laterally confined, and relies on the fact that at the transition from hillslopes to channels, the concentration of the flow increases both on a local and zonal scale.

We tested CO²CHAIN on four basins spanning low to high erosion rates, in which we have asked six geomorphologists to locate channel heads based on visual inspection of the LiDAR DEMs. Compared to two other state-of-the-art automatic methods, CO²CHAIN allows to better account for the average characteristics as well as the variability of channel head location, without the need to recalibrate the method for each basin.

2. Data Sources

In order to test CO²CHAIN across various settings, we have chosen four basins for which we could retrieve a LiDAR DEM and a long-term erosion rate based on cosmogenic radionuclides (¹⁰Be). They are located in the United States and in France and differ in terms of erosion rates, lithologies as well as morphology (e.g., degree of dissection and roughness, see Figure S1 in Supporting Information S1). The San Bernardino Mountains (SB) basin in California (Yucaipa Ridge 3 in Binnie et al. (2007)) is a fast eroding basin (1.18 mm/yr) in a granitoid massif. It has a very patchy soil cover and mostly exhibits rough bedrock. The San Gabriel Mountains (SG) basin (DiBiase et al. (2010), SGB6) has an erosion rate of 0.45 mm/yr. Its soil cover is sometimes patchy, exposing the anorthosite bedrock. The Oregon Coast Range (OC) basin (Penserini et al. (2017), CRN 501) has an erosion rate of 0.12 mm/yr and is carved in sandstone. It is entirely forested. The Alpes-de-Haute-Provence (HP) basin (Godard et al. (2020), TV-N,O,P) erodes at a rate of 0.03 mm/yr. It is composed of unevenly consolidated conglomerates and is mostly soil covered.

3. Methods

CO²CHAIN first detects the transition from unconfined to confined flow on all flowpaths starting from the crests within the DEM by monitoring two variables that we call the local flow concentration and the upstream flow convergence. We obtain a preliminary channel network that we correct by removing erroneous channel heads.

3.1. Channel Heads Extraction With CO²CHAIN

3.1.1. Processing the DEM

We use 1-m LiDAR-derived DEMs of small (1–10 km²) basins. We process them using the Matlab Topotoolbox (Schwanghart & Scherler, 2014). First, for 1-m resolution DEMs, we resample them to a resolution of 3 m using bi-linear interpolation. We then filter the DEM in order to remove meter-scale irregularities, which are indeed likely to be fallen boulders or uprooted trees that are erased by long term processes such as hillslope diffusion and sediment transport by rivers and debris flows. We therefore apply the Wiener filter included in the Topotoolbox.

3.1.2. Extracting the Crests Within the DEM

We first need to extract all the pixels corresponding to crests in the basin. The first criterion to identify the crests is the drainage area. We selected the pixels that have a drainage area of only one pixel according to a D8 algorithm, that is, those that do not have any upstream contributor. This includes isolated pixels that are higher than all their immediate neighbors but do not belong to any crest. To remove them, we impose an additional criterion based on a topographic position index (TPI) threshold. We define the TPI of one pixel as the difference between its elevation and the mean elevation of the DEM within a radius of 50 m. We select the pixels with a TPI over 0.5. This threshold has been adjusted to maximize the number of pixels belonging to crests by verifying that even some pixels manifestly not belonging to crests were kept. This allows to keep even the smallest crests, so that every potential channel can be extracted (Figure S2 in Supporting Information S1).

3.1.3. Hillslope/Channel Transition

3.1.3.1. Extracting All Possible Flowpaths

The next step consists in extracting each flowpath starting from the crest pixels and in identifying the transitions from hillslopes to channels. We use a D8 routing algorithm to extract these flowpaths. Around 90% of the basin is covered by the flowpaths starting from all the crest pixels (Figure S2 in Supporting Information S1). One out of two pixels can be discarded for efficiency without affecting the results.

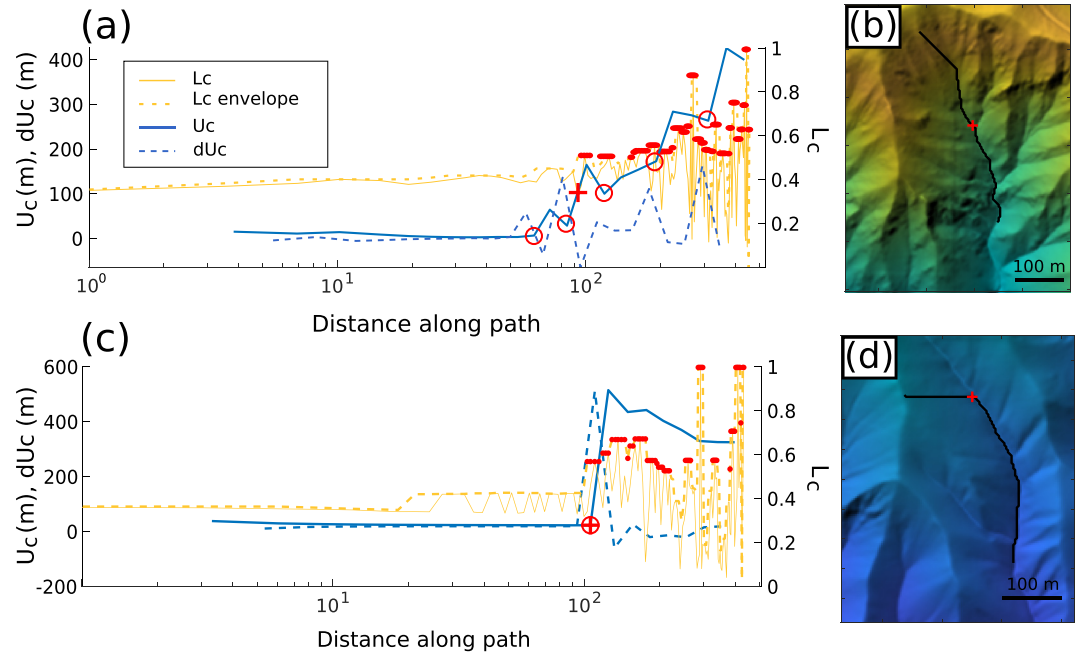


Figure 1. Flow convergence U_c and local flow concentration L_c along two flowpaths in the SG basin, resampled to 3 m. Continuous and dashed blue lines represent respectively the flow convergence and its derivative, yellow lines are local flow concentration and dashed yellow lines are their upper envelope calculated as explained in the text. Red circles indicate significant convergence jumps and the red dotted line indicates pixels where the local flow concentration envelope is above a certain threshold ($L_c^* = 0.5$ here). The maps on the right side show the flowpath on the DEM. The red cross is the pixel identified as the hillslope/channel transition. The red crosses indicate the location of the transition found by the method.

3.1.3.2. Local and Integral Metrics of Convergence

Since we define channels as laterally confined flow areas, we consider two variables which characterize convergence at an integrated or local scale. We expect these two variables to increase at the transition from distributed to confined flow. We combine two thresholds for these variables to locate this transition. We define the first variable as the upstream flow convergence, and the second one as the local flow concentration.

The upstream flow convergence is the ratio of the upstream drainage area of a considered pixel, A , to the flowpath length between the ridge and this pixel, D .

$$U_c = \frac{A}{D} \quad (1)$$

We compute A using the D-infinity flow direction algorithm described by Tarboton (1997) because it allows for finer quantification of flow emergence on gradually converging slopes. We observed that the transition from a hillslope to a channel is characterized by a large step-increase of U_c . However, local variations in high-resolution DEMs generate high frequency variations and short length discrepancies of U_c due to the differences in the two algorithms we use (D8 for flowpath and D-infinity for drainage area). In order to better identify the largest steps of U_c , we bin it logarithmically along the flowpath. In order to have the same bin distribution for every flowpath of every basin, we limit the flowpath length to 400 m downstream from the ridge, which is longer than the length of all the hillslopes in our basins. We then define 30 bins along the path and set the bin U_c value to the median of U_c on all pixels included in the bin. This allows us to derive a less noisy U_c and improves the identification of steps (Figure 1).

The local flow concentration, L_c , is the fraction of the flow that is distributed to the lowest neighboring pixel by a multiple flow algorithm computed following the method of Qin et al. (2007). In a well-entrenched channel, we expect L_c to reach one, whereas on a planar hillslope we expect $L_c \sim 0.3$ because flow must be distributed between three downslope pixels (Figure 1c). L_c is also very noisy, especially in channels or valleys broader than one pixel. At one pixel, the steepest slope is not necessarily oriented exactly toward one of the eight surround-

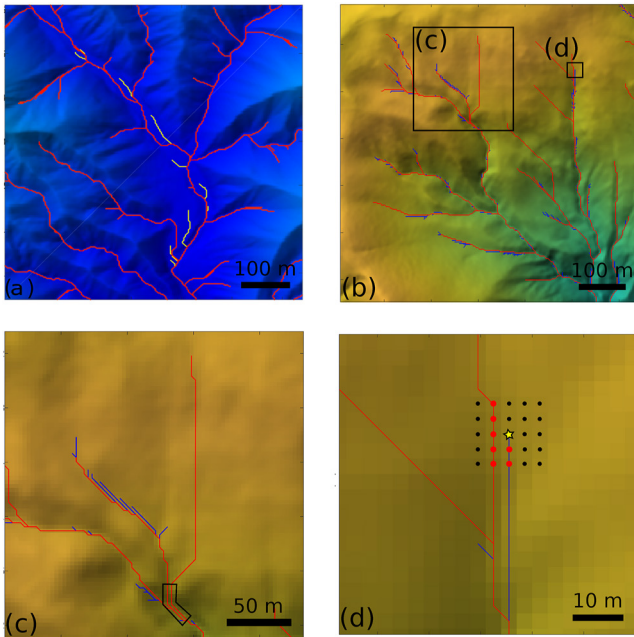


Figure 2. Correcting the channel network. Results of CO²CHAIN on a DEM resampled to 3 m in the SG basin. On all panels, the corrected network is red and the raw results are yellow or blue. Panel (a) shows the elimination of the channel heads located on the floodplain. Panels (b–d) show the elimination of the multiple channel heads at the top of the basins: all the blue segments are removed either because they are shorter than 20 m or through the systematic scanning of neighboring channel heads. Panel (c) shows another configuration where two adjacent channels should probably be merged: the part where they run alongside each other is circled in black. Panel (d) shows which pixels are investigated around a channel head (highlighted by the yellow star). Since eight of them are channel pixels (the red ones), the blue path is removed.

ing pixels and this can lower a lot the concentration value. Therefore L_c is sensitive to every slight change in the steepest slope direction. We avoid this problem by considering the upper envelope of the downstream curve of L_c , which corresponds to flow concentration on pixels where the steepest slope points toward one of the eight neighbor pixels. We simply compute the envelope by picking out for every pixel the maximum of flow concentration in a window of 15 m centered around the pixel on the flowpath. We chose this window size because we observed that L_c maxima varies at this length scale.

3.1.3.3. Hillslope/Channel Transition From Flow Convergence and Concentration

In order to locate the transition from hillslope to channel, we focus on joint variations of U_c and L_c along flowpaths. We isolated two different cases (Figure 1). The first case (Figures 1a and 1b) is when the flow path is situated at the top of a zero-order basin. L_c and U_c therefore change gradually near the transition. The second case (Figures 1c and 1d) is when a lateral planar hillslope directly ends in a well-formed channel. L_c and U_c then exhibit a single abrupt step at the transition. The initial and final values of U_c and the magnitude of the step are highly variable depending on where the flowpath is situated between these two end-members and on the local roughness of the DEM. This variability prevents us from defining an absolute threshold of U_c to define a channel.

Instead, we use a statistical threshold based on the upstream (hillslope) variability of U_c . At each bin, we compute the convergence change with respect to the previous bin dU_c as well as the mean and standard deviation of dU_c from the beginning of the flowpath to the current bin ($\overline{dU_c}$ and σ_{dU_c}). We consider that dU_c is statistically different from the upstream portion (and thus may be associated with the hillslope-channel transition) when:

$$dU_c \geq \overline{dU_c} + k^* \sigma_{dU_c}. \quad (2)$$

where k^* is a constant that needs to be calibrated (see Section 3.2). Similarly, we calibrate a threshold of L_c , L_c^* , such that the desired transition corresponds to $L_c = L_c^*$.

Preliminary tests showed that the two criteria do not perform well on their own since some small scale roughness in the DEM can cause independent variations in both metrics. Instead, where both an upstream flow convergence and local concentration steps are found at the same place, it is highly likely that it corresponds to a channel head. Therefore, we locate the first bin satisfying Equation 2 and located less than 15 m away from a pixel where the envelope of L_c exceeds L_c^* (Figure 1), and then identify the pixel with the largest dU_c within this bin. To do this, we must find all the significant U_c steps (Equation 2), based on the value of σ_{dU_c} found at the first step. Fixing σ_{dU_c} is required to find the following steps because after the first step the upstream standard deviation increases drastically making following variations of dU_c insignificant.

3.1.4. Channel Network Correction

Despite the combination of two channelization criteria, not all of the channel heads found with these criteria are geomorphologically meaningful. We have to apply three different corrections: removing heads on floodplains, removing duplicate channel heads and removing small parallel features branching on channels in a feather-like pattern.

Channel heads appear on floodplains because the D8 routing algorithm concentrates all the flow in a single pixel, leaving the wider floodplains out of the main flowpath. Therefore, it is possible that the transition from lateral slope to floodplain is wrongly characterized as a channel head (Figure 2a). We remove all channel heads with elevation and slope gradient below the 10th and 20th percentiles of the whole DEM distribution, respectively. This efficiently removes channel heads in floodplains but not elsewhere (Figure 2a).

Upstream, several channel heads are often identified for only one channel (Figures 2b and 2c). Indeed, numerous flowpaths descending from one crest lead to the same channel but the transition does not occur exactly at the same pixel for each of them. This yields channel duplicates that immediately join the main channel. Similarly, the transition is not always detected at the same exact location for planar lateral hillslopes. This results in few-pixel-long features branching into the main channel (Figure 2c).

Removing all segments smaller than 20 m allows us to remove most duplicate channels. However, some of these features run alongside the main channel for several tens of meter before joining it and thus could not be corrected by this minimum length threshold. To correct these, we inspect all of the remaining channel heads and compute for each of them the number of channelized pixels in the 24 neighboring pixels (i.e., within a two pixels radius). For an isolated channel head, there are at most five channelized pixels in this area. Beyond five channelized pixels, we consider that there are two adjacent channels which should likely be the same one, and we remove the investigated channel head (Figure 2d). This might remove actual channels if they are really close, but this is a rare case. This correction is also resolution-dependent and we adapt it at lower resolutions.

Finally, duplicated channels may also occur further downstream but not close to the channel head, and will thus not be removed by our correction (Figure 2c). This may slightly increase channel density but is an issue that cannot be automatically treated without attributing a width larger than a single pixel to the channels, thus we did not try to correct these.

3.2. Threshold Calibration Based on Expert Mapping

3.2.1. Systematic Mapping of Channel Heads by Geomorphologists

One key point to be able to calibrate and evaluate the algorithm is to have data to compare it with. Channel extraction methods are often developed and verified on DEMs of basins where some channel heads have been precisely mapped in the field (Clubb et al., 2014; Sofia et al., 2011).

However, beyond its very time consuming nature, extensive field mapping of channel heads is unlikely to be satisfying in catchments with high erosion rates and stochastic processes such as debris flows, for at least two reasons. First, because in such catchments most channels may be intermittently active, and thus many hydrological criteria (such as flow or banks) may not apply. Second, because such catchments often display steep relief and difficult terrain simply preventing access to map channel headwaters (Clubb et al., 2014).

As an alternative, we propose a mapping based on independent inspection of a relief map by six geomorphologists considered as experts. We ask them to map all of the detectable channel heads on a hillshade map of the four studied basins. Since CO²CHAIN is designed to find areas of concentrated flow, considered as sites where channelized erosion processes occur (and not hillslope processes), we ask experts to look for the transition from diffuse slopes to a channel where flow is confined between two walls, independently of other criteria. Although the results reflect to some extent the perception of the experts, the combination of their results should draw out geomorphologically relevant features.

Since we expect different results for different grid resolutions, the mapping exercise was repeated at three grid resolutions: 3, 10 and 30 m. Note that the experts would click on a pixel with a limited precision, thus being sometimes slightly offset of the pixel with high flow concentration. We found the mean distance between the manually selected pixel and the pixel with the maximum drainage area in the vicinity to be 10 m. Thus, we look for the main flowpath (i.e., the flowpath receiving the maximum drainage area) in the chosen pixel surroundings within a radius of 10 m, and if the chosen pixel does not belong to this flowpath, we assign the head to the closest pixel which does.

3.2.2. Comparison of Expert Mapping and Automatic Extraction

We test CO²CHAIN by running 80 tests for each DEM with k^* ranging from 6 to 24 (Equation 2) and L_c^* ranging from 0.3 to 0.7. For each simulation, we compare the results with the experts' results using three different metrics: the drainage area distribution at channel heads, the drainage density, and the location of a few robust channel heads. As for the drainage density, we compute the quadratic distance between the expert results and CO²CHAIN method results, d , defined by:

$$d = \sqrt{\frac{1}{6} \sum_{i=1}^6 (Dd - Dd_i)^2} \quad (3)$$

Where Dd is the drainage density and Dd_i is the drainage density derived from each expert's results. We then normalize the value of the quadratic distance using the mean of the six experts' drainage density.

As for channelization drainage area, we compare the probability density functions (PDF). The number of channel heads in one basin is between 50 and 100, which is too few to reliably use classical similarity tests such as the Kolmogorov-Smirnov test (Massey Jr, 1951). Instead, we compute the overlapping area minus the separated area below both PDF curves. Our drainage area misfit metric is equal to one minus this difference. Therefore, it is equal to zero when the PDF are the same.

Finally, we identify zero-order basins where at least three experts identified a channel head, and define the barycenter of these experts' heads as robust heads. We count how many of them have been found by the method and compute the mean of the distances between the reference heads and the corresponding method channel heads. If a reference head has not been found, the distance is the length of the whole corresponding zero-order channel.

3.3. Comparison With Other Methods

To assess the skills of CO²CHAIN we compare it to two recent channel extraction methods that are implemented in the LSDTopoTools software (Clubb, Mudd, Milodowski, Grieve, & Hurst, 2017): the DrEICH and the Wiener methods.

The DrEICH method is process-based and extracts the fluvial channels based on their signature in chi-space and their contour curvature (Clubb et al., 2014). LSDTopoTools provides several adjustable parameters to calibrate the method. The ones that are specific to this method are the number of network junction over which to perform the chi-analysis and the concavity value of the river network. A pruning drainage area to remove channel heads under a certain drainage area and a minimum length required for a convex feature to be considered as a valley can also be set (Clubb & Mudd, 2019).

The Wiener method implemented in LSDTopoTools is inspired by the methods of Pelletier (2013) and Passalacqua et al. (2010) and was first used in Grieve, Mudd, Milodowski, et al. (2016). It is a geometric method which identifies the valley network in the same way as the DrEICH method, then extracts the channel network based on a tangential curvature threshold chosen based on the PDF of curvature in the basin and prunes the obtained network using a drainage area threshold. It can be calibrated using the two previously cited parameters that are not specific to the DrEICH method (Clubb & Mudd, 2019).

These two methods are specifically calibrated in LSDTopoTools for 1-m DEMs. We used their default parameters when running them on 1-m DEMs and recalibrated them using the same metrics as described earlier at lower resolutions.

4. Results

4.1. Channel Heads Identified by Experts

We start by assessing the level of agreement of the different experts in mapping channel heads (Figure 3). Indeed, for the expert mapping to be considered a good benchmark to evaluate automatic channel extraction methods, dispersion among experts must be minimal. Dispersion either occur because different experts place the channel head more or less upstream an identified valley, or simply because some topographic features may be considered a channel by some experts while discarded by others. This yields differences both in drainage density and channelization drainage area (Figure S3 in Supporting Information S1).

In the HP basin, robust channel heads (i.e., mapped by at least three experts) represent 60% of all heads, and the mean dispersion between experts around these robust heads is 16 m. Five experts identify almost always the same channels, and considering only them, the robust heads would represent 83% of all channel heads mapped, and drainage densities would range between 0.0036 and 0.044. Only one expert identifies significantly more subchannels and thus has a slightly higher Dd (0.0052 m⁻¹). In OC, robust heads represent 78% of channel heads with a mean dispersion of 11 m. However, the Dd values are more dispersed. Indeed some channels up to 100 m long are not mapped by every expert. We assume that this is due to the fact that the channel are less narrow and incised in this DEM. However, A_c distribution and drainage densities are still similar.

As for the two other basins, their drainage networks are less simple to map. Because their erosion rates are higher than the two first basins, the soil cover is patchy, with bare bedrock outcropping in several places, especially at

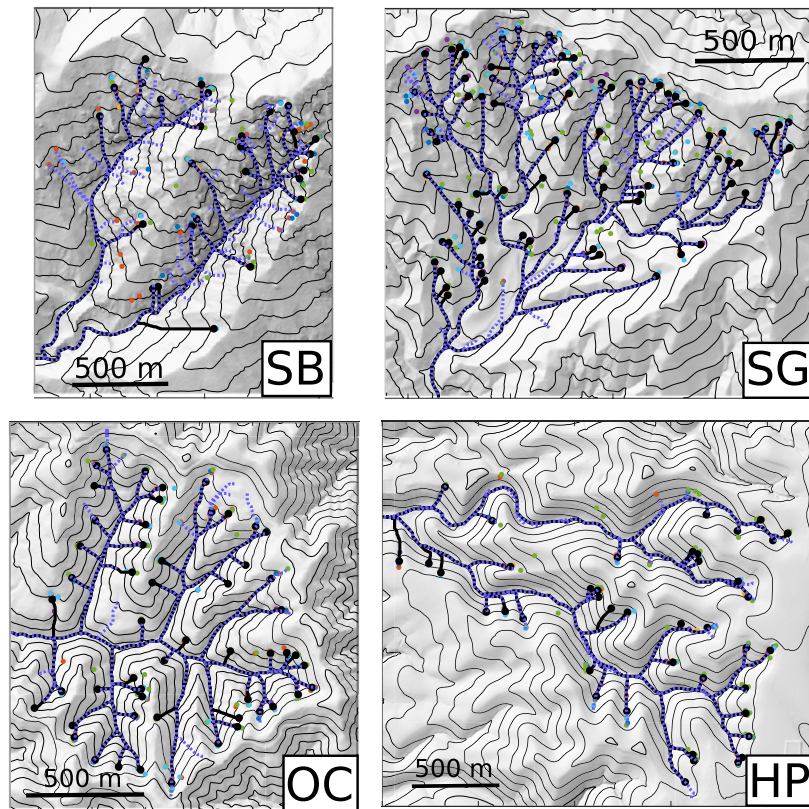


Figure 3. Channel heads mapped by the experts, robust drainage network and CO²CHAIN drainage network. The resolution of the DEMs is 3 m. The colored dots are the experts' mappings. Each color represents one person. The thick black lines represent the channel network extracted using the robust heads (i.e., mapped by at least three experts). The blue dashed lines are CO²CHAIN' channel networks.

the head of the basins. In these bedrock areas, especially in SB, channels are not well defined, leading to more disagreement among experts. As a result, robust heads represent 50% of all heads in SB with a mean dispersion of 18 m. This yields various drainage densities, ranging from 0.003 to 0.006 m⁻¹. In the SG basin, bedrock also outcrops in multiple places at the head of the basin. Furthermore, convergent slopes turn to channels in a very progressive fashion and not all channels are well defined. Consequently, some experts extract a lot more channels than others and the channel heads are placed at various drainage area. Nevertheless, robust heads represent 69% of all heads with a mean dispersion of 15 m. Five experts out of six found similar drainage densities (0.0065–0.0079 m⁻¹), and one found a significantly lower drainage density (0.0052 m⁻¹).

Overall, we find the statistics are close enough in the SG, OC and HP basins to consider the experts' mapping as a good benchmark to evaluate the accuracy of our automatic extraction method. We used it also in the SB basin, with the caveat that the expert's results are more dispersed.

4.2. Calibration of CO²CHAIN

We seek to calibrate CO²CHAIN by finding parameters that are not necessarily the optimal values for each basin, but give misfits that are close to the minimum for all three metrics of all basins. For three basins (SG, OC and HP), the best fitting parameters are in similar ranges, typically L_c^* between 0.4 and 0.5, and k^* between 8 and 14 even if the optimal value is slightly more variable. Therefore, we isolated a pair of parameters (12 for k^* and 0.45 for L_c^*) which satisfies our requirements.

As for the last basin (SB), the optimal parameters would be $L_c^* = 0.55$ and $k^* = 12$, however, this is the basin in which the experts disagreed the most. Consequently, we did not take into account these results to choose the optimal parameters. We will take a closer look at the results in the SB basin in the next section.

These results also show the sensitivity of CO²CHAIN to both thresholds, and show that in spite of some trade-off none of the tests are sufficient alone to extract a network similar to the one of the expert (Figure 4). The convergence step test allows to locate precisely where the transition occurs, while the local flow concentration test determines which potential transition is selected to be the channel head, and they are both equally essential.

4.3. Characteristics of the Drainage Network Obtained With CO²CHAIN

We ran CO²CHAIN in the four basins at a 3-m resolution using the best parameters found in the previous section. We then compared the channel heads extracted automatically to the ones mapped by the experts by looking at Dd , A_c distribution and robust channel heads location.

In the HP basin, 77% of the robust heads have been extracted by CO²CHAIN and the mean distance between these heads and the corresponding CO²CHAIN heads is 26 m. This yields a mean distance of 35 m when taking into account the robust heads that are not found. Some thin and poorly incised channels have been extracted by some experts and not by CO²CHAIN (Figure 3). Conversely, in spite of the corrections applied to the network, some spurious channels remain on the floodplain. As a result, Dd is almost identical to the mean of the experts (Figure 5). The median of A_c is also very close to the mean of the experts (94%).

In the OC basin, 82% of the robust heads have been identified with a mean distance of 27 m. This yields a mean distance of 30 m when taking into account the robust heads that are not found. Channels start mostly downstream or between the channel heads mapped by the experts, and more rarely upstream from them (Figure 3). Some features that have been considered as channel by several experts (between two and four out of six) are not detected by CO²CHAIN, because they are too wide to meet the local flow concentration criteria. Dd is still really close to the one of the experts (Figure 5). Since the channel heads of CO²CHAIN are mostly downstream or between the experts' ones, the median A_c is above (160%) the experts' mean.

In the SG basin, where the channels are more ambiguous, CO²CHAIN extracts most of the channels that have been mapped by at least three experts (67%), and the channel that are not extracted are mostly short channels (Figure 3). The mean distance between the experts' and CO²CHAIN channels is only 22 m. This yields a mean distance of 29 m when taking into account the robust heads that are not found. A lot of features that have been considered as channels by only one or two experts are extracted, thus Dd is close to the experts' mean. There does not seem to be a clear trend regarding whether channels start upstream or downstream from the experts (Figure 3), but the A_c distribution given by CO²CHAIN is also slightly shifted toward higher drainage areas compared to the experts' distribution (median A_c is 150% of the experts' mean).

In the SB basin, CO²CHAIN finds many more channels than the robust channel heads, resulting in a much higher (158%) Dd . 97% of the robust heads are found with a mean distance of 41 m, or 40 m when taking into account the robust heads that have not been found. However, we note that most of the channels extracted by CO²CHAIN have also been extracted by at least one expert. The A_c median is close to the one of the experts (120% of the experts' median A_c). Also, since all experts mapped different channels, we constructed a drainage network combining all of their channel heads (Figure S4 in Supporting Information S1). This network is close to the one found by CO²CHAIN and has a drainage density of 0.0072 m⁻¹ (95% of the CO²CHAIN method Dd). The best parameters to fit this combined data set are $L_c^* = 0.5$ and $k = 10$, but $L_c^* = 0.45$ and $k = 12$ also fits these results. In other words, if we consider that in this difficult terrain, the union of the experts gives a more accurate result than each of them taken separately (or their average), the threshold chosen for the three other basins would also be optimal for SB.

4.4. Slope-Area Scaling of Channel Heads Found by CO²CHAIN

We investigate the relationship between S and A for the channel heads extracted by the CO²CHAIN method (Figure 6). In SB, SG, and OC, channel heads have steep slopes (0.4–1) and 75% of them are located within a narrow domain defined by power-law functions of A ($S = (1.7 \pm 0.25)A^{-0.1}$). In HP there is no clear relationship between A and S , and only a few heads are in the power-law domain identified for the other basins. Our results concerning channel heads statistics can be biased by the fact that our correction does not eliminate all spurious channel heads on floodplains. However, this does not mean that the power law observed itself is biased: in the SG basin, for example, all of the remaining channel heads on floodplains (seven out of 87) are situated outside of the power law domain.

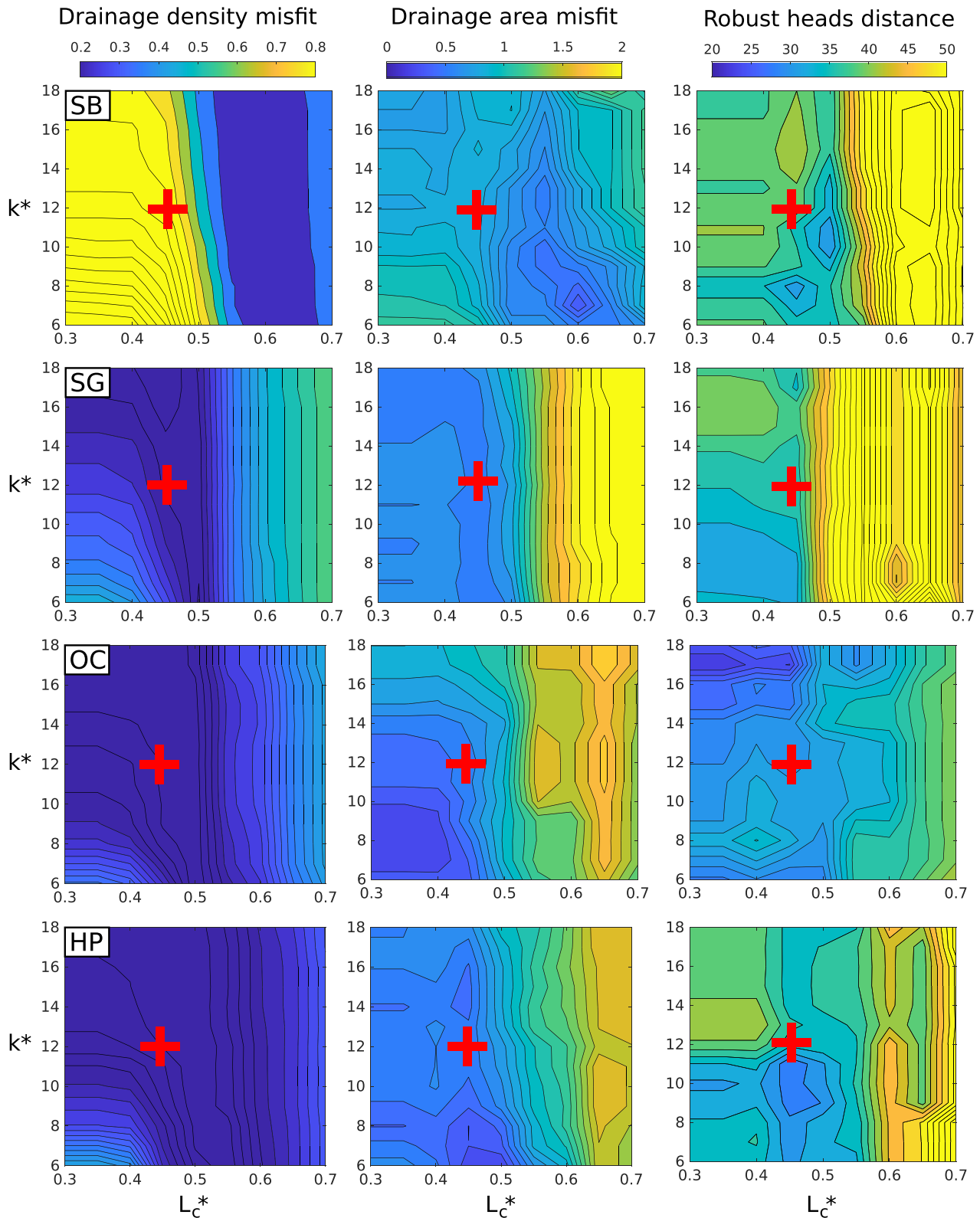


Figure 4. Misfit in drainage density and drainage area distribution and mean distance from the heads computed by CO²CHAIN to the ones deduced from the experts' mapping, computed as explained in Section 3.2.2. We run CO²CHAIN on 3-m resolution DEMs using different values for the thresholds. Vertical axis is the convergence change threshold k^* , given in number of standard deviations as explained in Section 3.1.3.3, and horizontal axis is the local flow concentration threshold L_c^* , without units. The red crosses show a set of parameters that give satisfying results for SG, OC, and HP basins.

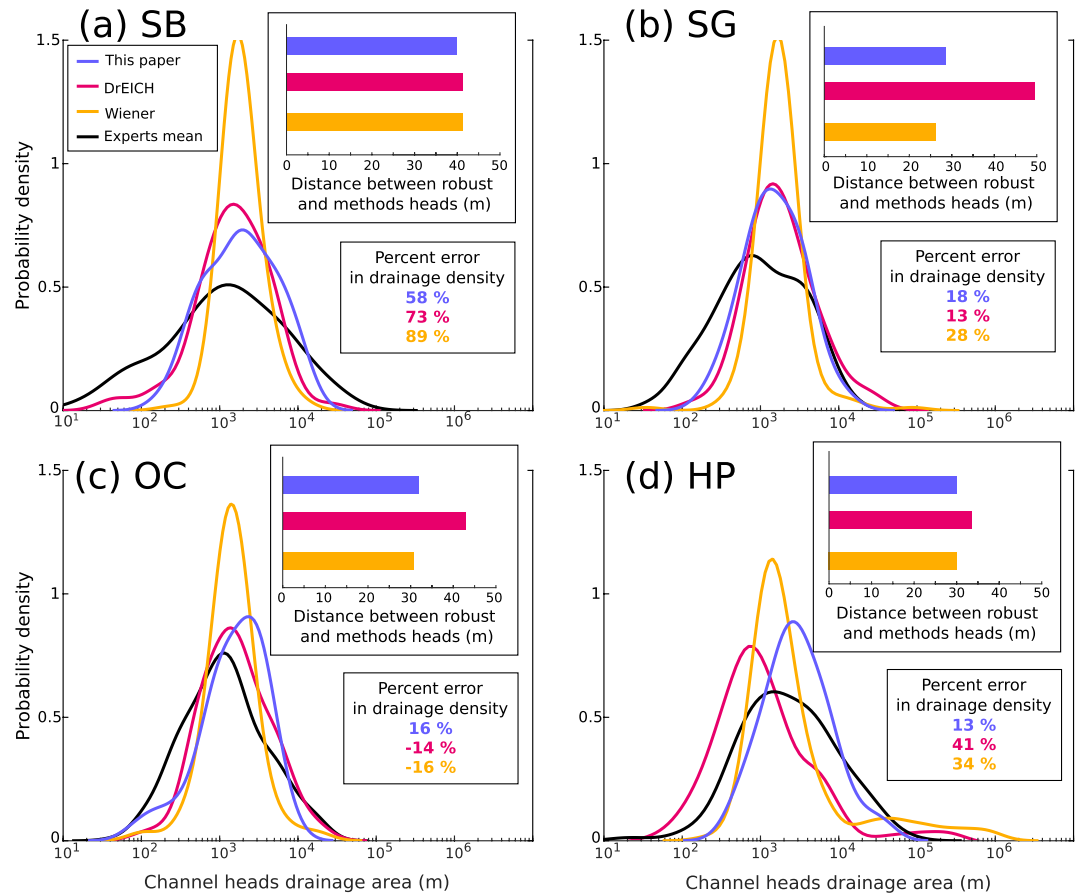


Figure 5. Comparison of drainage area, drainage density and channel heads location for the three automatic methods and the expert's mappings. The main plots refer to the A_c distribution and the insets show the drainage density misfit as well as the mean distance between channel heads extracted by the methods and the robust channel heads. Black: averaged experts' statistics, red: DrEICH, yellow: Wiener, blue: CO²CHAIN. CO²CHAIN was run on the DEMs resampled to 3 m and the other methods on the 1-m resolution DEM. The same parameters are used for all four DEMs (see Sections 4.2 and 4.4).

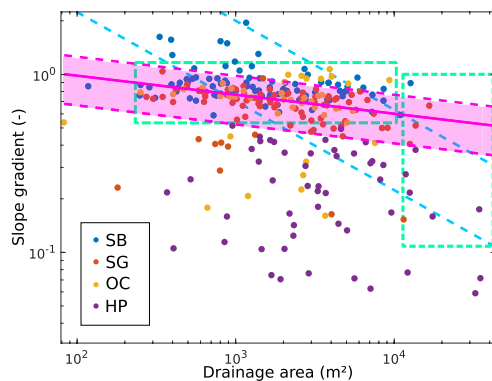


Figure 6. Channel heads slope-area relationship. The colored dots are the channel heads extracted using CO²CHAINS in the four DEMs resampled to 3 m. The pink solid line and pink domain is the best fitting power law for the SB, SG and OC basins ($S = 1.7 \pm 0.25 A^{-0.1}$). The blue dashed lines delimit the power law domain found by Montgomery and Dietrich (1992). It is bounded by two lines of equation $S = 63 A^{-0.5}$ and $S = 22 A^{-0.5}$. The green boxes show the results (without clear trends) of Clubb et al. (2014) using the DrEICH method on four LiDARs DEMs of four basins in the United States.

4.5. Results of the DrEICH and Wiener Methods

The Wiener and DrEICH channels are mostly calibrated for 1-m resolution DEMs, so we ran them on the original 1-m resolution DEMs with their default parameters which we found to fit the experts' results best. We only lowered the pruning drainage area of the DrEICH method to 500 m² to get better results.

We compared the drainage densities, drainage area distribution and location of robust heads for the four methods in each basin (Figure 5, Table S1 in Supporting Information S1). CO²CHAIN is more consistent than the two other methods regarding drainage density, since its misfit is systematically below 20% except in the SB basin, while the other methods have errors up to 30 or 40%. The drainage density misfits for all methods are higher in the SB basin, which was expected as discussed in Section 4.3.

The main differences appear in the two other metrics. Indeed, the Wiener method is highly affected by its pruning drainage area of 1,000 m² (see Figure S5 in Supporting Information S1 for the results with a pruning drainage area of 500 m²), and its drainage area distribution is similar to the one of a drainage area threshold, with a much smaller dispersion than the experts and two other methods. The DrEICH method appears to have the longest

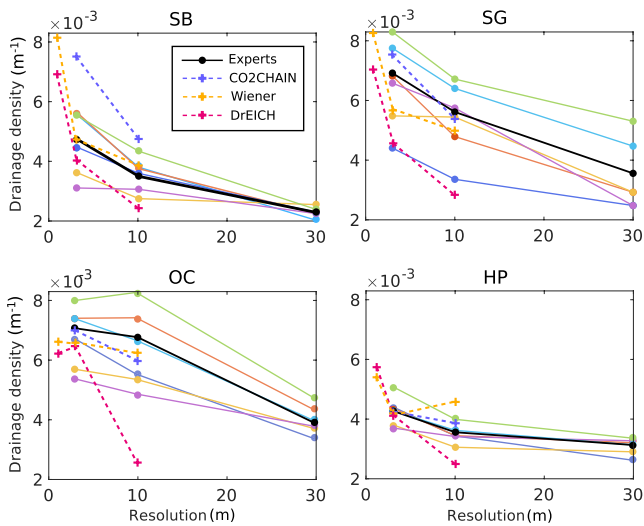


Figure 7. Drainage density of the drainage extracted by the six experts and by the three methods as a function of grid resolution. Each color line represents one expert, the colors being the same as on the maps of Figure 3. The discontinuous lines are the results of the three methods.

mean distance to the robust heads. It finds approximately the same amount of these robust heads as the other methods, but locates them mostly downstream of the experts, especially in the OC and SG basins, while the CO²CHAIN and Wiener methods have mean distances around 30 m taking into account the heads that have not been found, which is not much above the mean distance in between the experts. What allows DrEICH to fit well the experts' drainage area distribution is that it finds many channel heads at low drainage areas placed on curved hillslopes not considered as channels by any expert (False positives in Table S1 in Supporting Information S1). The match in distribution of channel heads area is therefore quite misleading in this case.

However, we noticed an issue with the “number of tributary junctions downstream,” N_t , a LSDTopotools parameter, which defines the lowermost point from which DrEICH will operate (Clubb & Mudd, 2019). At its default value of one, best-fitting the experts' results, the results in high-erosion catchments are not related anymore to an actual change of slope in the Chi-Z domain, but almost entirely determined by the algorithm finding zero-order valley location (Figure S6 in Supporting Information S1 discussion). In other words, for $N_t = 1$ and high-erosion rate, this implementation of DrEICH may not be called “process-based,” and to retrieve process-based fluvial heads we have had to set $N_t = 3$.

4.6. Effect of DEM Grid Resolution on the Methods

Although their availability is increasing, high-resolution DEMs are still limited to relatively few locations covered by LiDAR surveys. In most other places DEM resolution is limited to five, 10 or 30 m. This affects the drainage network retrieved by different extraction methods. As resolution decreases, channelized features with characteristic scale smaller than the resolution disappear from the DEMs, and thus cannot be retrieved by any method. Furthermore, different channel extraction methods are likely to perform variably, depending on the resolution, since the criteria they use (curvature, drainage area, slope...) are affected by resolution (Grieve, Mudd, Milodowski, et al., 2016).

As some features visually disappear of the DEMs when resolution decreases, the drainage density computed from the experts' mapping decreases when resolution decreases from 3 to 30 m (Figure 7). Depending on the characteristic scale of the low order channels, this trend can be more or less pronounced. Between resolutions of 3 to 10 m, the drainage densities computed from the experts' mapping in the HP, SB and to a lesser extent SG basins strongly decrease because many low order channels are thinner than 10 m in these basins, while they are often larger than that in the OC basin, in which Dd is much less affected by this resolution change. At a resolution of 30 m, Dd significantly drops for all basins.

Grieve, Mudd, Milodowski, et al. (2016) tested the DrEICH and Wiener method on DEMs at different resolutions and compared the results to those obtained at 1-m resolution. They found that the density of the drainage network steadily decreases with decreasing resolution for the two methods, but that Dd decreases faster when using the DrEICH method. They also showed that up to 10-m resolution the location of the channel heads found is still accurate enough for both methods. Our results on one, three and ten-m resolution DEMs confirm these trends (Figure 7; Figures S7 and S8 in Supporting Information S1). Indeed, between 3 and 10 m, the Wiener method is similarly affected by the resolution change as the experts are, while the DrEICH method results have a much lower drainage density and higher drainage area than the experts at a resolution of 10 m. Additionally, between 1 and 3 m, we found that the results of the DrEICH and Wiener methods deteriorate more in high-resolution DEMs (Figure 7, Supporting Information S1 discussion).

As for CO²CHAIN, between 3 and 10 m, the sensitivity of drainage density to resolution is slightly higher than the Wiener method, but much lower than the DrEICH method (Figure 7). On the contrary, A_c (which is related to channel head location) is less sensitive to resolution when using CO²CHAIN than the two other methods (Figure 7; Figure S7 in Supporting Information S1). Since the location of channel heads is determined by the convergence step in CO²CHAIN and by curvature in the Wiener method, this could be due to the

fact that curvature on small scale features is more sensitive to resolution than drainage area (Grieve, Mudd, Milodowski, et al., 2016; Wu et al., 2008). As a result, it seems that when resolution increases, CO²CHAIN finds fewer tributaries than the Wiener method, but detects the head of the remaining channels with more precision.

At a 1-m resolution, CO²CHAIN does not accurately locate channel heads and seems very sensitive to small scale roughness. We recommend to use this method on 3 m resampled DEMs, since it gives results that are as accurate or more accurate as the two other methods in 1-m resolution DEMs (Figure 5).

5. Discussion

5.1. Advantages and Limits of CO²CHAIN

CO²CHAIN appears to be able to give reliable results with the same parameters on basins ranging from low to high erosion rates, without requiring prior knowledge on them. We compared CO²CHAIN to two state-of-the-art methods, DrEICH and Wiener. CO²CHAIN is the only method that manage to fit at the same time drainage density, drainage area distribution and robust heads location. Its strong points are mainly the drainage density and channel heads drainage area distribution. It misses more robust heads than the two other methods (see Table S1 in Supporting Information S1) but locates them as accurately. Furthermore, it also finds a much fewer false positives (i.e., heads that have not been mapped by any expert).

Since the DrEICH method is meant to identify the upstream limit of the fluvial network, when there are colluvial channels and the number of junctions N_r is set to one, the channel head extraction is not process-based anymore but mainly relies on the identification of zero-order valleys (Figure S6 in Supporting Information S1 analysis). Thus it struggles to find the accurate location of channel heads, especially in high erosion rate basins, and detects channels on curved slopes.

The Wiener method gives accurate results in all basins in terms of drainage density and location of robust heads. However it seems to be heavily affected by the pruning drainage area. The drainage area distribution of channel heads systematically has a mean value just above the pruning drainage area set in LSDTopoTools and a much lower variance than the results of the experts (Figure 5 and Figure S5 in Supporting Information S1).

In comparison to Wiener, CO²CHAIN is not targeting a local property threshold such as contour curvature but rather a change of properties along the flowpath. Given this focus on a local property change relative to its value in the hillslope portion of the DEM, it may require less user adjustment when changing landscape or resolution. The local flow concentration threshold L_c^* remains an absolute value parameter, which did not need to be tuned for the four studied catchments. Still the stability of L_c^* on a broader range of catchments remains to be assessed.

One-meter resolution topographic data is not available everywhere. At a slightly lower resolution (3 m), the results of Dreich and Wiener methods are degraded on the two high-erosion catchments and become worst than CO²CHAIN (Figure S7 in Supporting Information S1).

The main limitation of CO²CHAIN is the scale limit it imposes on channels. First, it is yet unable to extract channel heads in 1-m resolution DEMs, and thus cannot retrieve channels in landscape where their characteristic scale is less than 3 m. The corrections applied to the network also introduce scale limits. The first one is the length of zero-order channels, which must be at least 20 m, and the second one is the spacing between channels, which must be at least 9 m. This is a choice we made to avoid having to impose a drainage area threshold. This way, small features can be overlooked but the location and drainage area signature of channel heads is preserved.

CO²CHAIN also does not handle the fact that occasionally incipient channels can disappear within fans or other unchannelized portions of the landscape. Thus, a future improvement could be to handle this as done by Pelletier (2013), after identifying heads and before constructing the final network. Finally, the spurious channel heads situated on floodplains are not all eliminated. In the HP basin, 10 out of the 41 channel heads extracted by the CO²CHAIN method are located on floodplains, and in the other basins a few channel heads also remain on floodplains. This does not affect much the drainage network itself and its drainage density, but can distort the channel head slope and area statistics. Furthermore, the current correction can remove actual channels that flow on the floodplain. CO²CHAIN may benefit from being coupled with algorithms able to detect floodplains (Clubb, Mudd, Milodowski, Valters, et al., 2017) and thus to eliminate spurious heads in this domain.

5.2. Perspectives for Revisiting Slope-Area Scaling for Channel Heads

CO²CHAIN may allow to revisit what controls the transition from non-channelized processes on the hillslopes to channelized processes, including when debris-flows happen. While many physically based studies have been conducted to define a channel initiation criterion linking the drainage area at the channel head, A , to its slope S (Dietrich & Dunne, 1993; Dietrich et al., 2020; Kirkby, 1986), only few field data appeared to support predictions (Montgomery & Dietrich, 1988, 1992), while also being very noisy possibly because of fine-scale variability of surface conditions (Istanbulluoglu et al., 2002). Recent analysis on high-resolution DEMs did not find any relation between S and A (Clubb et al., 2014).

CO²CHAIN was optimized based on the expert mapping who developed their expertise on global morphology and had little chance to structure their results around a specific $S - A$ relationship. The weakly negative power law we find for the channel heads extracted by CO²CHAIN (Figure 6) is thus likely the signature of a specific competition between geomorphic processes (Tucker & Bras, 1998) different from the ones identified by Montgomery and Dietrich (1992), namely subsurface flow and shallow landsliding. In SG and OC field observations showed that debris flows contribute to bedrock channel incision (DiBiase & Lamb, 2020; Penserini et al., 2017), and more generally laboratory experiments and theoretical work suggest that in channel with such gradients (>0.5 , Figure 6) bedload transport is less likely than en masse failure of sediments on the bed (Prancevic et al., 2014). Thus, we suggest that debris flows are likely one of the processes contributing to the channel head signature we observe, and encourage efforts toward a more detailed understanding of the competition shaping the hillslope to channel transition at high erosion rates, including various processes such as landslides and debris flows among others.

In HP, the absence of correlation between slope and area is difficult to interpret but may be related to a diversity of processes, including possibly rilling. Additionally, at least some of the channel heads near the main divide may be either influenced by progressive retrogression into the Puymichel Plateau or may be influenced by sapping in relation to subsurface water flow (Berhanu et al., 2012). Last, we cannot exclude that the very weak nature of the conglomerate rocks in the area (Godard et al., 2020) is also leading to specific channel initiation conditions, increasing scatter.

5.3. Insights on Valley Heads Morphology and Catchment Drainage Density

Our method locates channels heads which are inherently ill-defined features, especially in areas where channels are not always filled with water. However, the approximate location of channel heads allows to delimit the broader area representing the head of valleys, which captures the progressive transition from hillslopes to channels. One of the quantities which characterize the shape of the basin head is the convergence U_c , as described in Equation 1. At the scale of individual flowpaths, due to the short scale irregularities and the discrepancies between the D8 flow routing algorithm and the D-infinity drainage area computation, the value of U_c along the flowpath and across the transition is very noisy (Figure 1), hence the need for local concentration to better identify the transition. However, we may gain insight by studying the change of U_c along flowpath, averaged for all the channel heads of a given catchment.

We compute the evolution of U_c along the longest flowpath between the hilltop and each channel head, defining a normalized distance, $D^* = D/D_T$, where D_T is the distance at the channel head. We stack all flowpaths in each study area to retrieve the mean of the convergence profile in valley heads (Figure 8a).

For each basin, it has a sigmoidal shape, with an inflexion point located around the channelization zone. This scaling break supports our idea that the CO²CHAIN method detects an actual change of regime in the water and sediment transport, from diffused to confined.

Furthermore, differences between convergence curves may reflect differences in the morphology and processes operating in the valley heads of each basin. In the HP basin e.g., slopes are less convergent and channels are more convergent than in the other basins, resulting in a sharper transition at the channel head (Figure 8). The hillshade map of the basin (see Figure 3) shows that slopes are not much convergent, especially those starting on the Valensole plateau at the East of the basin. The transition between hillslopes and channel is also very sharp. Conversely, the SB basin convergence evolution exhibits channels that are less convergent and the hillslope to channel transition is thus less sharp, which is also consistent with the basin appearance (Figure 3), where channels originate in

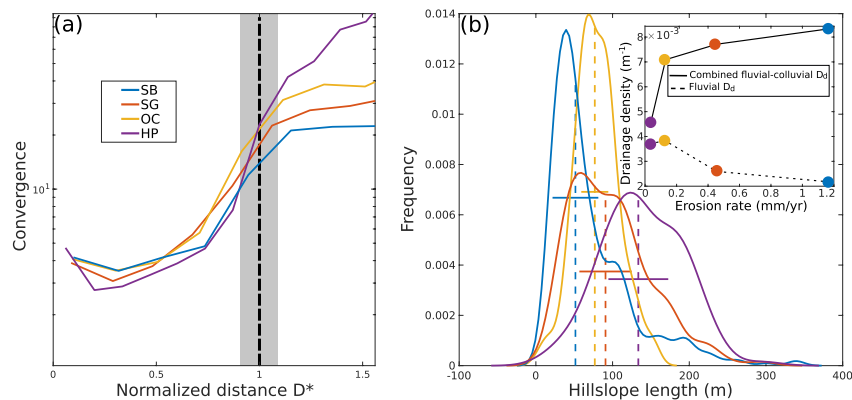


Figure 8. Hillslopes length and convergence. Panel (a) shows the evolution of the convergence value (U_c) along the slopes at the head of zero-order basins in our four basins. Each curve represents the median of the convergence of all the zero-order valleys in one DEM. The distance along the slopes is normalized by the distance from the crest to the hillslope/channel transition retrieved by CO²CHAIN in the basins resampled to 3 m. The vertical line at $D^* = 1$ and gray area is the channelization zone. Panel (b) shows the length statistics of the hillslopes at the head of zero-order streams for each basin. The inset is the fluvial and total drainage density of each basin.

small, steep-sided valleys with rough slopes. The evolution of convergence at valley heads could thus be a novel statistical indicator of the shape of valley heads and possibly of process shaping them.

This also allows to revisit studies on hillslope length such as the one of Grieve, Mudd, and Hurst (2016). In their study, hillslopes are extracted from all hilltops pixels, contrary to here where hillslopes are extracted only at the head of zero-order valleys. Their length statistics are more dispersed than what we find and their slopes are longer in average (Figure 8b). Extracting hillslope statistics only at valley heads might be more relevant to understand the transition from hillslope processes to channelized processes.

Hillslope lengths appear to generally decrease as the average catchment erosion rate increases (Figure 8b). This is equivalent to say that the combined fluvial-colluvial drainage density is increasing with erosion rate (Figure 8b). Such increase may be explained by the stream power-law with $n > 1$ (Clubb et al., 2016), but given the presence of colluvial channels in the studied area (e.g., OC and SG, DiBiase et al., 2012; Penserini et al., 2017; Stock & Dietrich, 2003) we rather interpret it as caused by increased activity (or efficiency) of colluvial processes such as debris-flows. In contrast, applying the DrEICH method with the number of junction set to three yields a channel network likely more aligned with fluvial processes, with a lower and slightly decreasing drainage density across basins (Figure 8b). Such results complete those of DiBiase et al. (2012), who identified manually debris-flow channels start and end, and found a constant combined fluvial-colluvial drainage density and a reduction of the fluvial drainage density with increasing erosion rates. However, the main difference is that we compare four catchments with different climatic, tectonic and lithological contexts which may create spurious trends with erosion rate. Nevertheless, CO²CHAIN, combined with DrEICH, unlocks a path toward systematic extraction of colluvial and fluvial drainage density and of the properties of the colluvial channels in a large number of catchments.

6. Conclusions

We have developed a new automatic channel extraction method, CO²CHAIN, designed to detect channels in high-resolution DEMs, regardless of their process of formation. CO²CHAIN is based on the detection of significant increases of two different convergence metrics along all possible flowpaths of one catchment. CO²CHAIN was calibrated against mapping carried out by geomorphologists on four basins covering a wide range of erosion rates, lithology, soil cover and erosion processes. We compared its results to that of two state-of-the-art channel extraction methods (DrEICH and Wiener methods).

We found that CO²CHAIN can consistently retrieve colluvial and fluvial channel heads in high and low erosion rate catchments, using two threshold for the convergence metrics: $L_c^* = 0.45$ and $U_c^* = 12$. Out of the three methods we tested, only CO²CHAIN could fit at the same time drainage density, drainage area distribution and

channel heads location. These results suggest that CO²CHAIN can be used on any basin regardless of the erosion processes and the erosion rate. It is also less affected by erosion rate than the two other methods at lower resolutions such as 3 m.

However, CO²CHAIN is not suitable for short scale features and imposes scale thresholds in terms of channel length and spacing between channels. Calibrating it for 1-m resolution DEMs could help reduce these thresholds.

We computed the slope-area relationship of channel heads as well as the dependence of drainage density on erosion rates in the four basins, and these results seem promising to revisit previous studies on channel heads and drainage network properties, especially on fastly eroding basins in which these studies have rarely been conducted. This could be an important step to understand long-term erosion by colluvial processes such as debris flows and include them in landscape evolution models (McGuire et al., 2022).

Conflict of Interest

The authors declare no conflicts of interest relevant to this study.

Data Availability Statement

All the DEMs used are available online. The San Bernardino Mountains, San Gabriel Mountains and Oregon Coast Range basins are found on the OpenTopography website (DOGAMI, 2011; Heimsath et al., 2019; Milodowski, 2014). The Haute Provence basin comes from the RGE-alti@database (<https://geoservices.ign.fr/rgealti>) (IGN, 2014). The codes for the CO²CHAIN method are available online (Lurin, 2023).

Acknowledgments

The author thank Mikael Attal, Jon Pelletier and an anonymous reviewer for handling and reviewing in details the manuscript. We thank Simon Mudd, Fiona Clubb and Boris Gailleton for their help on using LSDTopoTools, Vincent Godard for his help to access the Haute Provence DEM as well as Wolfgang Schwanghart for developing and distributing the Matlab TopoTool-Box. All four author contributed to the manual channel mapping as well as Remi Bossis and Anne Guyez who are warmly thanked. AL and OM conceived the study and developed the methodology with input from PM and SC. AL performed all analysis and code development and wrote the manuscript, under the supervision of OM and SC.

References

- Berhanu, M., Petroff, A., Devauchelle, O., Kudrolli, A., & Rothman, D. H. (2012). Shape and dynamics of seepage erosion in a horizontal granular bed. *Physical Review*, 86(4), 041304. <https://doi.org/10.1103/physreve.86.041304>
- Binnie, S. A., Phillips, W. M., Summerfield, M. A., & Fifield, L. K. (2007). Tectonic uplift, threshold hillslopes, and denudation rates in a developing mountain range. *Geology*, 35(8), 743–746. <https://doi.org/10.1130/g23641a.1>
- Chorley, R. J., & Morgan, M. (1962). Comparison of morphometric features, Unaka Mountains, Tennessee and North Carolina, and Dartmoor, England. *Geological Society of America Bulletin*, 73(1), 17–34. [https://doi.org/10.1130/0016-7606\(1962\)73\[17:comfum\]2.0.co;2](https://doi.org/10.1130/0016-7606(1962)73[17:comfum]2.0.co;2)
- Clubb, F. J., & Mudd, S. M. (2019). User guide to channel extraction using lsdtopotools. Retrieved from https://lsdtopotools.github.io/LSDTT_documentation/LSDTT_channel_extraction.html
- Clubb, F. J., Mudd, S. M., Attal, M., Milodowski, D. T., & Grieve, S. W. (2016). The relationship between drainage density, erosion rate, and hilltop curvature: Implications for sediment transport processes. *Journal of Geophysical Research: Earth Surface*, 121(10), 1724–1745. <https://doi.org/10.1002/2015JF003747>
- Clubb, F. J., Mudd, S. M., Milodowski, D. T., Grieve, S. W., & Hurst, M. D. (2017). Lsdchannextraction v 1.0 [Software]. Zenodo. <https://doi.org/10.5281/zenodo.824198>
- Clubb, F. J., Mudd, S. M., Milodowski, D. T., Hurst, M. D., & Slater, L. J. (2014). Objective extraction of channel heads from high-resolution topographic data. *Water Resources Research*, 50(5), 4283–4304. <https://doi.org/10.1002/2013wr015167>
- Clubb, F. J., Mudd, S. M., Milodowski, D. T., Valters, D. A., Slater, L. J., Hurst, M. D., & Limaye, A. B. (2017). Geomorphometric delineation of floodplains and terraces from objectively defined topographic thresholds. *Earth Surface Dynamics*, 5(3), 369–385. <https://doi.org/10.5194/esurf-5-369-2017>
- DiBiase, R. A., Heimsath, A. M., & Whipple, K. X. (2012). Hillslope response to tectonic forcing in threshold landscapes. *Earth Surface Processes and Landforms*, 37(8), 855–865. <https://doi.org/10.1002/esp.3205>
- DiBiase, R. A., & Lamb, M. P. (2020). Dry sediment loading of headwater channels fuels post-wildfire debris flows in bedrock landscapes. *Geology*, 48(2), 189–193. <https://doi.org/10.1130/g46847.1>
- DiBiase, R. A., Whipple, K., Heimsath, A., & Ouimet, W. (2010). Landscape form and millennial erosion rates in the San Gabriel Mountains, CA. *Earth and Planetary Science Letters*, 289(1–2), 134–144. <https://doi.org/10.1016/j.epsl.2009.10.036>
- Dietrich, W. E., & Dunne, T. (1993). The channel head. *Channel Network Hydrology*, 175, 219.
- Dietrich, W. E., Wilson, C. J., & Reneau, S. L. (2020). Hollows, colluvium, and landslides in soil-mantled landscapes. In *Hillslope processes* (pp. 362–388). Routledge.
- DOGAMI. (2011). Oregon department of geology and mineral industries lidar program data [Dataset]. OpenTopography. <https://doi.org/10.5069/G9QC01D1>
- Doyle, M. W., & Harbor, J. M. (2003). Modelling the effect of form and profile adjustments on channel equilibrium timescales. *Earth Surface Processes and Landforms*, 28(12), 1271–1287. <https://doi.org/10.1002/esp.516>
- Gilbert, G. K. (1909). The convexity of hilltops. *The Journal of Geology*, 17(4), 344–350. <https://doi.org/10.1086/621620>
- Godard, V., Hippolyte, J.-C., Cushing, E., Espurt, N., Fleury, J., Bellier, O., et al. (2020). Hillslope denudation and morphologic response to a rock uplift gradient. *Earth Surface Dynamics*, 8(2), 221–243. <https://doi.org/10.5194/esurf-8-221-2020>
- Grieve, S. W., Mudd, S. M., & Hurst, M. D. (2016). How long is a hillslope? *Earth Surface Processes and Landforms*, 41(8), 1039–1054. <https://doi.org/10.1002/esp.3884>
- Grieve, S. W., Mudd, S. M., Milodowski, D. T., Clubb, F. J., & Furbish, D. J. (2016). How does grid-resolution modulate the topographic expression of geomorphic processes? *Earth Surface Dynamics*, 4(3), 627–653. <https://doi.org/10.5194/esurf-4-627-2016>

- Hattajji, T., Kodama, R., Takahashi, D., Tanaka, Y., Doshida, S., & Furuichi, T. (2021). Migration of channel heads by storm events in two granitic mountain basins, western Japan: Implication for predicting location of landslides. *Geomorphology*, 393, 107943. <https://doi.org/10.1016/j.geomorph.2021.107943>
- Heimsath, A., Hudnut, K., Lamb, M., & Whipple, K. (2019). Mapping of San Gabriel Mountains, CA 2009 fire [Dataset]. OpenTopography. <https://doi.org/10.5069/G94M92N4>
- Hergarten, S., Robl, J., & Stüwe, K. (2016). Tectonic geomorphology at small catchment sizes—extensions of the stream-power approach and the χ method. *Earth Surface Dynamics*, 4(1), 1–9. <https://doi.org/10.5194/esurf-4-1-2016>
- Horton, R. E. (1945). Erosional development of streams and their drainage basins; hydrophysical approach to quantitative morphology. *Geological Society of America Bulletin*, 56(3), 275–370. [https://doi.org/10.1130/0016-7606\(1945\)56\[275:edosat\]2.0.co;2](https://doi.org/10.1130/0016-7606(1945)56[275:edosat]2.0.co;2)
- IGN. (2014). Composante altimétrique du rge © [dataset]. Géoservices. Retrieved from <https://geoservices.ign.fr/>
- Istanbulluoglu, E., Tarboton, D. G., Pack, R. T., & Luce, C. (2002). A probabilistic approach for channel initiation. *Water Resources Research*, 38(12), 61–1. <https://doi.org/10.1029/2001wr000782>
- Izumi, R., & Parker, G. (2000). Linear stability analysis of channel inception: Downstream-driven theory. *Journal of Fluid Mechanics*, 419, 239–262. <https://doi.org/10.1017/s002211200001427>
- Kirkby, M. (1986). A runoff simulation model based on hillslope topography. In *Scale problems in hydrology* (pp. 39–56). Springer.
- Lague, D. (2014). The stream power river incision model: Evidence, theory and beyond. *Earth Surface Processes and Landforms*, 39(1), 38–61. <https://doi.org/10.1002/esp.3462>
- Leopold, L. B., & Miller, J. P. (1956). *Ephemeral streams: Hydraulic factors and their relation to the drainage net* (Vol. 282). US Government Printing Office.
- Loewenherz, D. S. (1991). Stability and the initiation of channelized surface drainage: A reassessment of the short wavelength limit. *Journal of Geophysical Research*, 96(B5), 8453–8464. <https://doi.org/10.1029/90jb02704>
- Lurin, A. (2023). Audlu/CO²CHAIN: CO²CHAIN. [Software]. Zenodo. <https://doi.org/10.5281/zenodo.8226515>
- Massey, F. J., Jr. (1951). The Kolmogorov-Smirnov test for goodness of fit. *Journal of the American Statistical Association*, 46(253), 68–78. <https://doi.org/10.1080/01621459.1951.10500769>
- McCoy, S. W., Kean, J. W., Coe, J. A., Staley, D. M., Wasklewicz, T. A., & Tucker, G. E. (2010). Evolution of a natural debris flow: In situ measurements of flow dynamics, video imagery, and terrestrial laser scanning. *Geology*, 38(8), 735–738. <https://doi.org/10.1130/g30928.1>
- McGuire, L. A., McCoy, S. W., Marc, O., Struble, W., & Barnhart, K. R. (2022). Steady-state forms of channel profiles shaped by debris-flow and fluvial processes. *Earth Surface Dynamics Discussions*, 1–33.
- Milodowski, D. (2014). Yucaipa ridge, San Bernardino Mountains, CA [Dataset]. OpenTopography. <https://doi.org/10.5069/G93T9F55>
- Montgomery, D. R., & Dietrich, W. E. (1992). Channel initiation and the problem of landscape scale. *Science*, 255(5046), 826–830. <https://doi.org/10.1126/science.255.5046.826>
- Montgomery, D. R., & Dietrich, W. E. (1988). Where do channels begin. *Nature*, 336(6196), 231–233. <https://doi.org/10.1038/336232a0>
- O'Callaghan, J. F., & Mark, D. M. (1984). The extraction of drainage networks from digital elevation data. *Computer Vision, Graphics, and Image Processing*, 28(3), 323–344. [https://doi.org/10.1016/s0734-189x\(84\)80047-x](https://doi.org/10.1016/s0734-189x(84)80047-x)
- Orlandini, S., Tarolli, P., Moretti, G., & Dalla Fontana, G. (2011). On the prediction of channel heads in a complex alpine terrain using gridded elevation data. *Water Resources Research*, 47(2). <https://doi.org/10.1029/2010wr009648>
- Pallard, B., Castellarin, A., & Montanari, A. (2009). A look at the links between drainage density and flood statistics. *Hydrology and Earth System Sciences*, 13(7), 1019–1029. <https://doi.org/10.5194/hess-13-1019-2009>
- Passalacqua, P., Do Trung, T., Foufoula-Georgiou, E., Sapiro, G., & Dietrich, W. E. (2010). A geometric framework for channel network extraction from lidar: Nonlinear diffusion and geodesic paths. *Journal of Geophysical Research*, 115(F1), F01002. <https://doi.org/10.1029/2009jf001254>
- Pelletier, J. D. (2013). A robust, two-parameter method for the extraction of drainage networks from high-resolution digital elevation models (DEMs): Evaluation using synthetic and real-world DEMs. *Water Resources Research*, 49(1), 75–89. <https://doi.org/10.1029/2012wr012452>
- Penserini, B. D., Roering, J. J., & Streig, A. (2017). A morphologic proxy for debris flow erosion with application to the earthquake deformation cycle, Cascadia Subduction Zone, USA. *Geomorphology*, 282, 150–161. <https://doi.org/10.1016/j.geomorph.2017.01.018>
- Perron, J. T., Dietrich, W. E., & Kirchner, J. W. (2008). Controls on the spacing of first-order valleys. *Journal of Geophysical Research*, 113(F4), F04016. <https://doi.org/10.1029/2007JF000977>
- Perron, J. T., Richardson, P. W., Ferrier, K. L., & Lapôtte, M. (2012). The root of branching river networks. *Nature*, 492(7427), 100–103. <https://doi.org/10.1038/nature11672>
- Perron, J. T., & Royden, L. (2013). An integral approach to Bedrock river profile analysis. *Earth Surface Processes and Landforms*, 38(6), 570–576. <https://doi.org/10.1002/esp.3302>
- Prancevic, J. P., Lamb, M. P., & Fuller, B. M. (2014). Incipient sediment motion across the river to debris-flow transition. *Geology*, 42(3), 191–194. <https://doi.org/10.1130/G34927.1>
- Qin, C., Zhu, A.-X., Pei, T., Li, B., Zhou, C., & Yang, L. (2007). An adaptive approach to selecting a flow-partition exponent for a multiple-flow-direction algorithm. *International Journal of Geographical Information Science*, 21(4), 443–458. <https://doi.org/10.1080/13658810601073240>
- Roering, J. J., Kirchner, J. W., & Dietrich, W. E. (1999). Evidence for nonlinear, diffusive sediment transport on hillslopes and implications for landscape morphology. *Water Resources Research*, 35(3), 853–870. <https://doi.org/10.1029/1998wr900090>
- Schwanghart, W., & Scherler, D. (2014). Topotoolbox 2—MATLAB-based software for topographic analysis and modeling in earth surface sciences. *Earth Surface Dynamics*, 2(1), 1–7. <https://doi.org/10.5194/esurf-2-1-2014>
- Shelef, E., & Hilley, G. E. (2016). A unified framework for modeling landscape evolution by discrete flows. *Journal of Geophysical Research: Earth Surface*, 121(5), 816–842. <https://doi.org/10.1002/2015JF003693>
- Smith, T. R., & Bretherton, F. P. (1972). Stability and the conservation of mass in drainage basin evolution. *Water Resources Research*, 8(6), 1506–1529. <https://doi.org/10.1029/wr008i006p01506>
- Sofia, G., Tarolli, P., Cazorzi, F., & Dalla Fontana, G. (2011). An objective approach for feature extraction: Distribution analysis and statistical descriptors for scale choice and channel network identification. *Hydrology and Earth System Sciences*, 15(5), 1387–1402. <https://doi.org/10.5194/hess-15-1387-2011>
- Stock, J., & Dietrich, W. E. (2003). Valley incision by debris flows: Evidence of a topographic signature. *Water Resources Research*, 39(4). <https://doi.org/10.1029/2001WR001057>
- Stock, J. D., & Dietrich, W. E. (2006). Erosion of steepland valleys by debris flows. *GSA Bulletin*, 118(9–10), 1125–1148. <https://doi.org/10.1130/B25902.1>
- Tarboton, D. G. (1997). A new method for the determination of flow directions and upslope areas in grid digital elevation models. *Water Resources Research*, 33(2), 309–319. <https://doi.org/10.1029/96wr03137>

- Tarboton, D. G., & Ames, D. P. (2001). Advances in the mapping of flow networks from digital elevation data. In *Bridging the gap: Meeting the world's water and environmental resources challenges* (pp. 1–10).
- Tarboton, D. G., Bras, R. L., & Rodriguez-Iturbe, I. (1992). A physical basis for drainage density. *Geomorphology*, 5(1–2), 59–76. [https://doi.org/10.1016/0169-555x\(92\)90058-v](https://doi.org/10.1016/0169-555x(92)90058-v)
- Tucker, G. E., & Bras, R. L. (1998). Hillslope processes, drainage density, and landscape morphology. *Water Resources Research*, 34(10), 2751–2764. <https://doi.org/10.1029/98wr01474>
- Whipple, K. X., Kirby, E., & Brocklehurst, S. H. (1999). Geomorphic limits to climate-induced increases in topographic relief. *Nature*, 401(6748), 39–43. <https://doi.org/10.1038/43375>
- Willgoose, G., Bras, R. L., & Rodriguez-Iturbe, I. (1991). A coupled channel network growth and hillslope evolution model 1. Theory. *Water Resources Research*, 27(7), 1671–1684. <https://doi.org/10.1029/91wr00935>
- Wu, W., Fan, Y., Wang, Z., & Liu, H. (2008). Assessing effects of digital elevation model resolutions on soil–landscape correlations in a hilly area. *Agriculture, Ecosystems & Environment*, 126(3–4), 209–216. <https://doi.org/10.1016/j.agee.2008.01.026>